Current Applied Physics 17 (2017) 1401–1408

Contents lists available at ScienceDirect

Current Applied Physics

journal homepage: www.elsevier.com/locate/cap

Flexible transparent electrodes made of core-shell-structured carbon/metal hybrid nanofiber mesh films fabricated via electrospinning and electroplating

Jin Woo Huh [a], Hwan-Jin Jeon [b, *], Chi Won Ahn [a, **]

[a] Department of Nano-Structured Materials Research, National NanoFab Center (NNFC), 291 Daehak-ro, Yuseong-gu, Daejeon 34141, Republic of Korea
[b] Department of Chemical Engineering and Biotechnology, Korea Polytechnic University, 237 Sangidaehak-ro, Siheung-si, Gyeonggi-do 15073, Republic of Korea

ARTICLE INFO

Article history:
Received 7 June 2017
Received in revised form
30 July 2017
Accepted 31 July 2017
Available online 3 August 2017

Keywords:
Core-shell structure
Carbon-metal hybrid
Flexible transparent electrode
Electrospinning
Electroplating

ABSTRACT

The development of practical flexible transparent electrodes is one of the major core technology fields for future nanoscale optoelectronics. Despite the many efforts to replace the indium tin oxide (ITO) electrode, preparing practical alternatives that satisfy the essential requirements of flexible transparent electrodes remains a challenge. In this work, core-shell-structured carbon/metal hybrid mesh (CS-CMHM) films, comprised of a metal layer coated onto conductive carbon nanofiber network structures, were fabricated using electrospinning and electroplating and demonstrated potential for use as flexible transparent electrodes. In contrast to previously described techniques that use conventional polymer fibers as sacrificial structures, the conductive carbon nanofibers used in the current technique that we developed provided bi-functionality: they formed conductive core channels and artificial supports of the metal structures. The CS-CMHM films displayed superior optoelectrical, mechanical, and thermal properties: they transmitted ~91% of visible light, showed a low sheet resistance of ~2.7 Ω/sq, and displayed excellent mechanical stability even after 10000 cycles of bending the films to a radius of 5 mm; also, applying a voltage of only 3 V to a transparent heater based on CS-CMHM films resulted in the temperature of the film surface increasing very rapidly in the first 20 s, and soon thereafter reaching ~280 °C. Based on these results, we believe that the use of CS-CMHM films and the process we developed to fabricate them open up great opportunities for high-performance flexible transparent electronics.
© 2017 Elsevier B.V. All rights reserved.

1. Introduction

Flexible transparent electrodes have attracted intensive attention in various existing and emerging applications, including future optoelectronic devices such as touch panels [1], organic light-emitting diodes [2,3], solar cells [4–6], wearable electronics [7–9], display devices [10] and automobile applications [11,12]. Developing transparent electrodes that combine low electrical resistance, high optical transmittance, and mechanical flexibility is an ultimate goal in this field. Indium tin oxide (ITO) has been the predominant commercial transparent electrode used in industry and applications since it provides an optimal tradeoff between resistance and transmittance and mechanical stability. However, its general use is critically limited by its rising cost due to the low abundance of indium; moreover, its application in practical flexible electronics is limited by its inherent brittleness.

As a result of these limitations, diverse ITO replacement candidates, such as carbon nanotubes (CNTs) [3,6,13,14], conducting polymers [5,15–17], graphene [1,18–20], metal nanowires [21–23], and metal nanofiber meshes [24–28] have been widely explored for application in flexible transparent conductors. Among them, metal meshes of electrospun metal nanofiber webs are considered to be particularly promising candidates: the electrospun nanofibers can span an extremely long distance with a continuous 1-dimensional (1-D) shape and realize highly uniform nanoscale metal networks with a low percolation threshold [29]; moreover, as a result of these properties, these meshes can achieve excellent optical transparency and electrical conductivity as well as flexibility when composed of nanosized metal structures.

Recently, many efforts have been made to develop high-

* Corresponding author.
** Corresponding author.
E-mail addresses: hjjeon@kpu.ac.kr (H.-J. Jeon), cwahn@nnfc.re.kr (C.W. Ahn).

http://dx.doi.org/10.1016/j.cap.2017.07.016
1567-1739/© 2017 Elsevier B.V. All rights reserved.

performance transparent electrodes by utilizing the electrospinning process for obtaining advanced interlinked nanofiber meshes. Cui's group [26,27] used electrospinning and metal deposition via thermal evaporation to fabricate a new type of highly flexible transparent electrode of metallic nanofiber networks. Although the network films displayed highly enhanced optoelectronic performance, the metal deposition method used to interconnect the nanofibers is a high-vacuum process and is not practical for low-cost production. Furthermore, the thermal post-treatment inhibits the wider use of flexible polymer-based substrates for flexible optoelectronics. In order to overcome these limitations, Yoon's group [28] introduced Cu-electroplated electrospun nanofiber mesh films, produced using low-temperature and non-vacuum processing. These films exhibited exceptional optoelectrical properties and mechanical stability due to the remarkably reduced contact resistance between intersecting fibers caused by their self-fused junctions formed by electroplating. However, despite the excellent optoelectrical properties of these films, multiple steps are required to make the fibers conductive for facilitating the electroplating, with these steps including adding supplementary Ag nanoparticles and depositing a noble-metal seed layer. Also note that the above-mentioned research groups employed electrospun polymer nanofiber templates used only as sacrificial frameworks for forming the metal fiber and that were fully removed or left in place without any use after coating of the metal layer. Hence, the resultant metal fibers showed hollow or polymer-filled tubes [28], or curved-ribbon structures [26], and such structures are apt to cause mechanical or thermal failures, resulting in electrical disconnection or thermal deformation of the fiber channels.

In this work, we developed a facile process to fabricate core-shell-structured carbon/metal hybrid mesh (CS-CMHM) films, composed of a metal layer covering conductive carbon nanofiber network structures, by combining electrospinning and electroplating. This developed technique is based on controlling the electroplating process to uniformly generate the metal layer on conductive carbon nanofiber seeds. Here, the conductive carbon nanofibers, which were processed using a heat treatment (carbonization), provided bi-functionality: they formed conductive core channels and artificial supports of the metal structures. In the investigations described below, we made technologically important advances to our technique for fabricating conducting core-shell nanostructures: (i) using this method, we were able to fabricate carbon-hybridized metal meshes with core-shell-structured (core: carbon fiber, shell: metal layer) nanofibers over a large area; (ii) these core-shell fiber webs enhanced the electrical, mechanical, and thermal properties of the films, which were shown to be due to the formation of core-area-packed carbon nanofibers having superior mechanical strength and high electrical and thermal conductivity; (iii) complex structures with various sizes were prepared by simply controlling the electrospinning and electroplating conditions; and (iv) we were able to fabricate freestanding transparent flexible thin films that we were able to apply, using the electroplating technique, onto complex surfaces of various metal materials.

To demonstrate this novel approach, core-shell-structured mesh films made of gold layer-coated carbon nanofibers were fabricated for use in flexible transparent electrodes. The resulting CS-CMHM films exhibited a high, ~91%, transmittance of light at a wavelength of 550 nm, a low sheet resistance of ~2.7 Ω/sq, and excellent mechanical stability even after 10000 cycles of bending to a radius of 5 mm. Additionally, a transparent heater consisting of the CS-CMHM films was demonstrated in high operating temperature. These results indicated a significant potential for the use of CS-CMHM films, and the efficient and facile method to make them, in high-performance flexible transparent electrodes and their applications.

2. Experimental

2.1. Fabrication of PAN precursor nanofiber meshes

Polymer mesh structures with nanosized fibers as a precursor of carbon nanofiber meshes (/templates) were prepared by electrospinning (Nano NC Co., Korea, ESN-HV30B) using a polyacrylonitrile (PAN, Mw = 1.5×10^5 g/mol, Sigma Aldrich) solution. PAN with a subunit molecular formula C3H3N can produce carbon fibers with a relatively high carbon yield [30]. The PAN solution was produced by dissolving PAN powder in dimethylformamide (DMF, Sigma-Aldrich), and solutions with 12 wt% PAN were used for fabricating nanosized polymer fibers. The dispersed PAN solution was transferred into a metal-tipped syringe (0.50 mm inner diameter, 21G). The parameters utilized for electrospinning were a pump rate of 0.3 mL/h and an electric field of 7 kV, and the distance between the needle tip and grounded collector was 13 cm. A square steel use stainless (SUS) frame with dimensions of 2.5 cm × 2.5 cm was used as the substrate for collecting the electrospun PAN nanofibers.

2.2. Carbonization, Au electroplating, and transfer to substrates

Carbon nanofiber meshes were produced by heating the electrospun PAN fibers with a two-step process consisting of thermal stabilization and carbonization. PAN precursor fiber webs previously prepared in the SUS frame were placed on an alumina boat and inserted in the heating zone of a furnace. The heating was carried out at 240 °C for 1 h in air (to effect stabilization) and then at 900 °C for 1 h in an Ar gas flow of 1.5 l/min (for carbonization). Next, an 8 wt% PAN solution was electrospun above the carbon nanofiber meshes using a pump rate of 0.3 ml/h at an applied voltage of 8 kV. These nanofibers sustained the carbon nanofiber webs and protected them from being damaged during electroplating. After that, the SUS frame containing collected carbon nanofibers was made to serve as a cathode by immersing it in an Au electroplating solution with a pure Pt anode, and a potential of 0.85–1 V was applied for ~3 min. The SUS frame was then rinsed with DI water. After the rinsing, the layers of PAN nanofibers which were supporting the carbon nanofiber webs were then removed by dissolving them in DMF. Then, finally, Au fiber meshes electroplated on the carbon fiber webs, i.e., the CS-CMHMs, were transferred onto a substrate such as glass and plastic films by spreading several drops of the DMF solution on the substrate. Once DMF evaporated from the substrates, the frame was then raised and removed.

2.3. Characterizations

The surface features and morphology of the CS-CMHMs were characterized by using field emission-scanning electron microscopy (FE-SEM) (Sirion FE-SEM, FEI), and the cross-sectional analysis of the CS-CMHMs was performed by focused ion beam (FIB) (Helios nanolab 600, FEI). The elemental distribution in the fibers was determined by acquiring energy dispersive spectroscopy (EDS) mapping scans. Sheet resistance was characterized by using a four-point probe system (Cascade Microtech, Inc.) with a source measure unit (4200-SCS, Keithley). Transmittance was recorded on a UV–visible/NIR spectrophotometer (Lambda 1050, PerkinElmer). Mechanical stability was analyzed using a bending test system. The system consisted of a two-contact interface serving to induce compressive stress to the sample, where one interface was fixed and immobile, while the other was allowed to move laterally using a motion controller (T-LSR075D, Zaber). The surface temperature of the mesh films resulting from Joule heating was measured by using an infrared (IR) camera (A305sc, FLIR) with a source measure unit (OPS-305, ODA).

3. Results and discussion

Fig. 1 shows the overall process, including electrospinning and electroplating, used to fabricate the CS-CMHM films. First, nano-sized PAN precursor polymer fiber networks were created as a framework by using a circular collector during electrospinning (Fig. 1a) and then assembled on an SUS frame to yield metal-electroplated fiber meshes (Fig. 1b). Following this assembly, in order to prepare carbon nanofiber meshes, the polymer nanofibers collected in the SUS frame were treated by heating them at 240 °C in air to stabilize them and then at 900 °C with an Ar flow to carbonize them (Fig. 1c). These heat treatments converted the PAN fiber precursors to carbon fibers. The stabilization process plays an important role in converting the PAN fiber to an infusible stable ladder polymer in which C≡N bonds are converted to C═N bonds [31], and allows the fibers to withstand the high temperature of the carbonization treatment [32]. Carbonization is in general an aromatic growth and polymerization process, in which the fiber is heated at a high temperature of up to or even over 800 °C, and typically yields an approximately 90% carbon content [33]. This heating process is found to produce a high tensile strength fiber. Next, electroplating was used to deposit Au on the carbon nanofiber templates (Fig. 1d). These Au-electroplated fiber meshes, i.e., CS-CMHMs, were then transferred to the desired substrates (Fig. 1e and f). Notably, we were able to successfully transfer the CS-CMHMs onto substrates due to the formation of physical contacts between the free-standing mesh structures and the substrates during the transfer process.

Fig. 2 shows the SEM images of the CS-CMHMs fabricated using electrospinning, followed by heat treatment, and then Au electroplating. As seen in the figure, electrospun PAN polymer nanofibers with diameters of ~700 nm were prepared (Fig. 2a), and carbonized nanofibers were successfully produced from the PAN precursor after the heat treatment (Fig. 2b). Notably, the carbon nanofibers were observed to have diameters of ~300–400 nm, approximately half those of the PAN nanofibers; we attributed this decrease to thermal shrinkage during the carbonization process [34]. In prior studies [35,36], a relationship between diameter, density and performance of carbon fibers during carbonization was investigated. Mittal et al. [35] observed that thinner carbon fibers were denser and mechanically stronger.

Trinquecoste et al. [36] also observed a high-tensile-strength fiber resulting from a carbonization heating process. Therefore, the decrease in the diameter observed in the carbon nanofibers we produced likely also increased their mechanical strength. Lastly, the CS-CMHMs were generated by electroplating Au on the surface of the carbon fiber templates (Fig. 2c–e). The figures show that the Au electroplating led to the formation of highly fused junctions at the intersections of the original carbon nanofibers.

Especially, the focused ion beam (FIB) cross sectional images in Fig. 2e clearly demonstrate that the covered Au layer is perfectly continuous without boundaries. This formation was attributed to the electroplated gold completing the imperfect junctions around the crossed carbon nanofibers, and ensured extremely low contact resistance at the junctions. Moreover, as shown in Fig. 2d–e, Au fibers naturally linked each other together and were randomly networked, which resulted from the electrospun fiber templates comprising well-woven fiber nets.

The morphology and composition of the fabricated carbon nanofibers and the CS-CMHMs were determined using SEM and

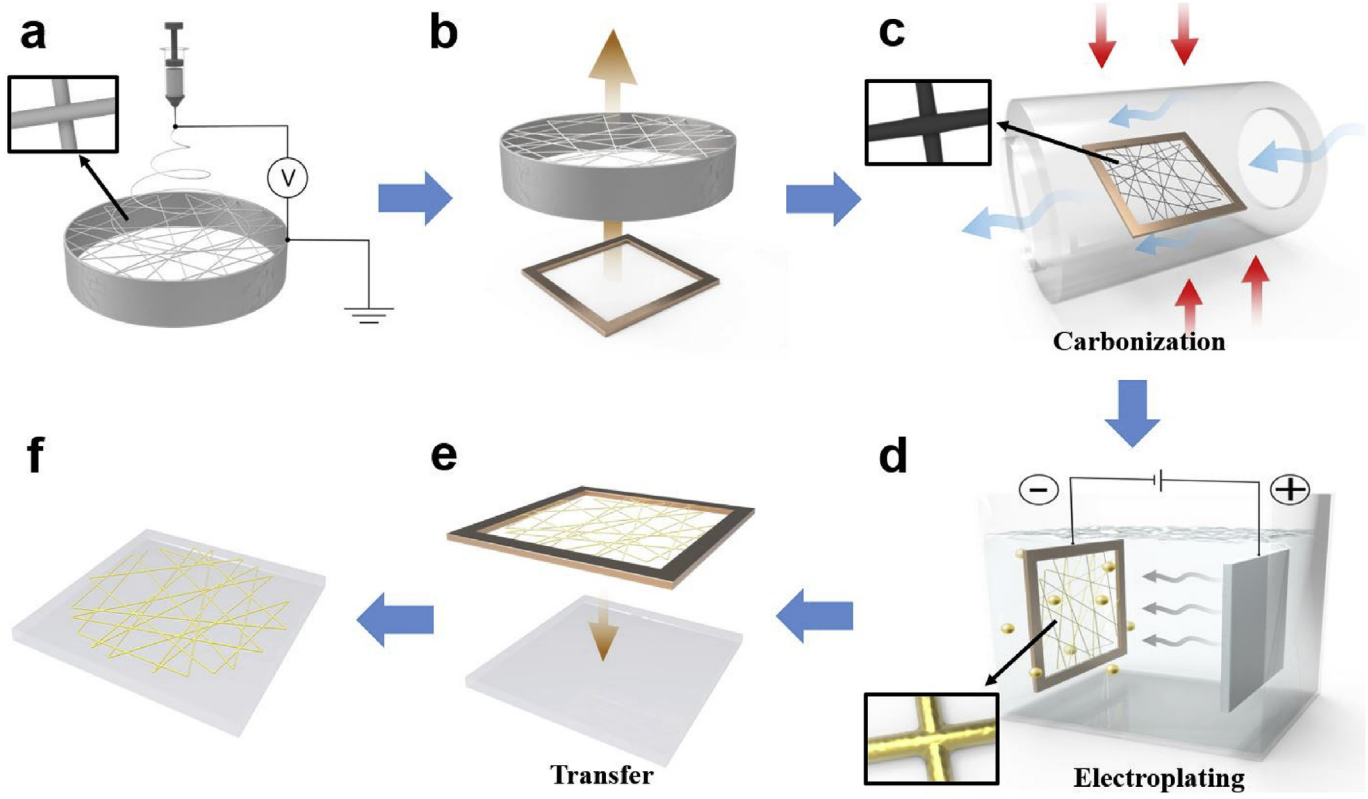

Fig. 1. Schematic of the process used to fabricate the core-shell-structured carbon/metal hybrid mesh (CS-CMHM) films. (a) Electrospinning was used to fabricate PAN nanofiber network precursors of the carbon nanofiber templates. (b) The electrospun fibers were gathered onto a SUS frame with a free-standing form. (c) Heating PAN nanofiber networks resulted in the formation of carbon nanofiber webs. (d) Au was electroplated onto the carbon nanofiber networks. (e,f) Finally, CS-CMHM structures were transferred onto substrates.

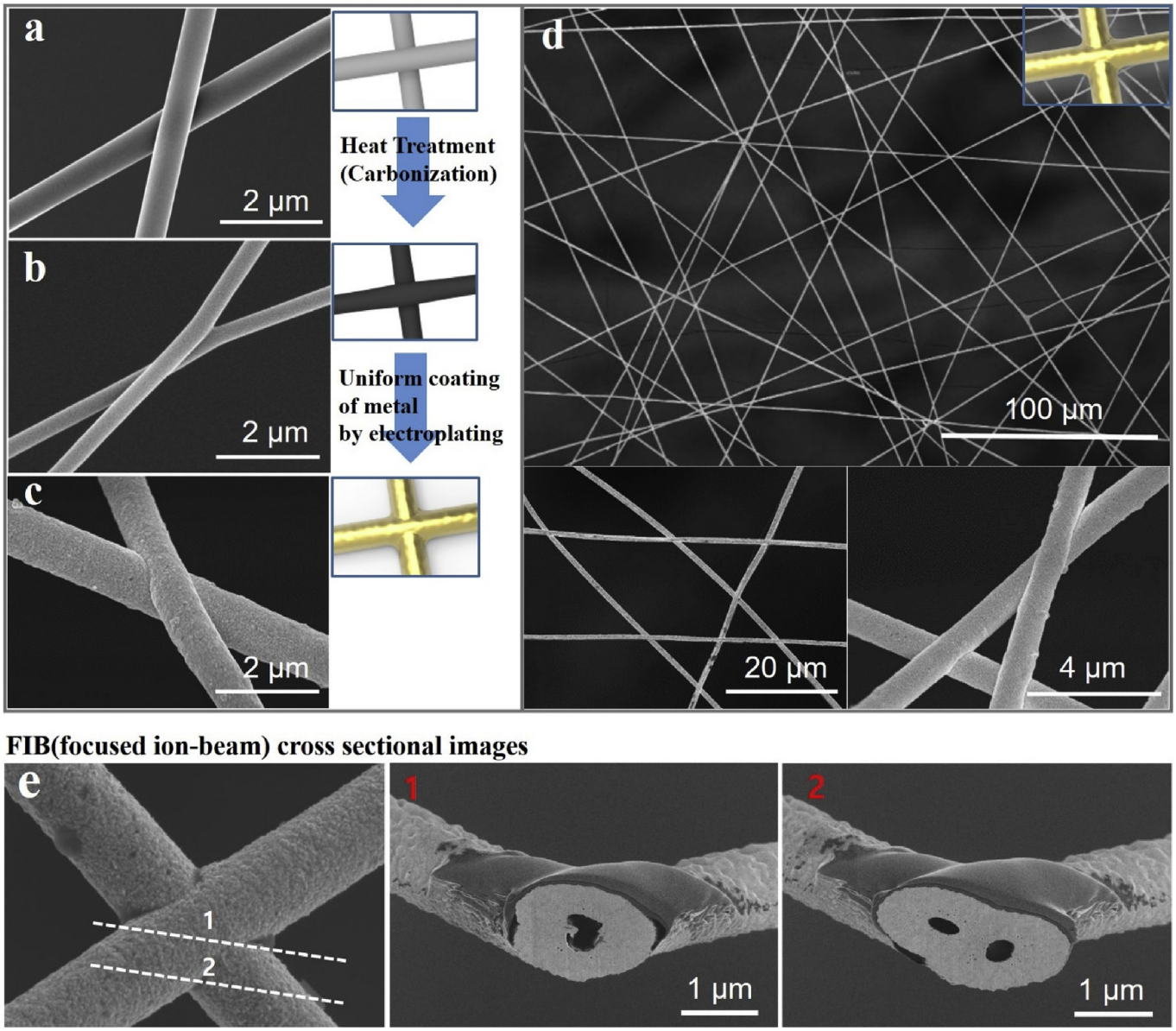

Fig. 2. SEM images of (a) PAN precursor nanofibers, (b) carbon nanofibers after heat treatment of the PAN precursor, (c) CS-CMHMs, which were fabricated by electroplating Au on the surface of the carbon nanofiber templates, and (d) CS-CMHMs at various magnifications. (e) Focused ion beam (FIB) cross sectional images at the intersections of the CS-CMHNs.

EDS. Their chemical compositions and element distributions were determined by acquiring EDS mapping scans, as shown in Fig. 3a. The SEM images showed the fabricated carbon nanofibers (left) as seed fibers and the corresponding core-shell-structured carbon/metal hybrid nanofibers (CS-CMHNs) after Au electroplating (right). The EDS mapping of the carbon fibers indicated as expected a dense distribution of the element carbon, with this distribution being consistent with the shapes of the fibers. This dense distribution coincided with the percentage of the fiber made up of carbon being over 80% according to the elemental analysis. The crystallization of the carbon nanofibers was also examined by using Raman spectroscopy (Fig. 3b). These nanofibers showed the typical two Raman carbon peaks: at about 1365 cm^{-1} and 1585 cm^{-1}, which are referred to, for carbon materials, as the D band and G band, respectively. The former was attributed to defect-inducing, i.e., noncrystalline, amorphous carbon and the latter to single crystals of graphite. The peak at the G band was observed to be more intense than that at the D band (Fig. 3b), indicating a relatively extensive formation of graphite-like crystals in the fabricated carbon nanofibers. Note that such graphite-like carbon structures are electrical conductors. The levels of dependence of this crystallization and corresponding electrical conductivity of the carbon nanofibers on carbonization temperature are shown in Supporting Information. The analysis of the CS-CMHNs using SEM and EDS mapping showed a uniform conformal coating of Au on the outer surface of the carbon nanofibers, with the EDS elemental analysis clearly verifying the presence of C and Au in the CS-CMHNs.

To determine how well our CS-CMHM films would perform as transparent electrodes, the electrical and optical properties of the films were investigated. Fig. 4a shows the transmittance of the CS-CMHMs and their seed templates, i.e., the carbon nanofiber meshes. For the carbon fiber meshes before being plated with Au, the percent transmittance of visible light and the sheet resistance were observed to be 96% (Fig. 4a) and ~7050 Ω/sq, respectively. The

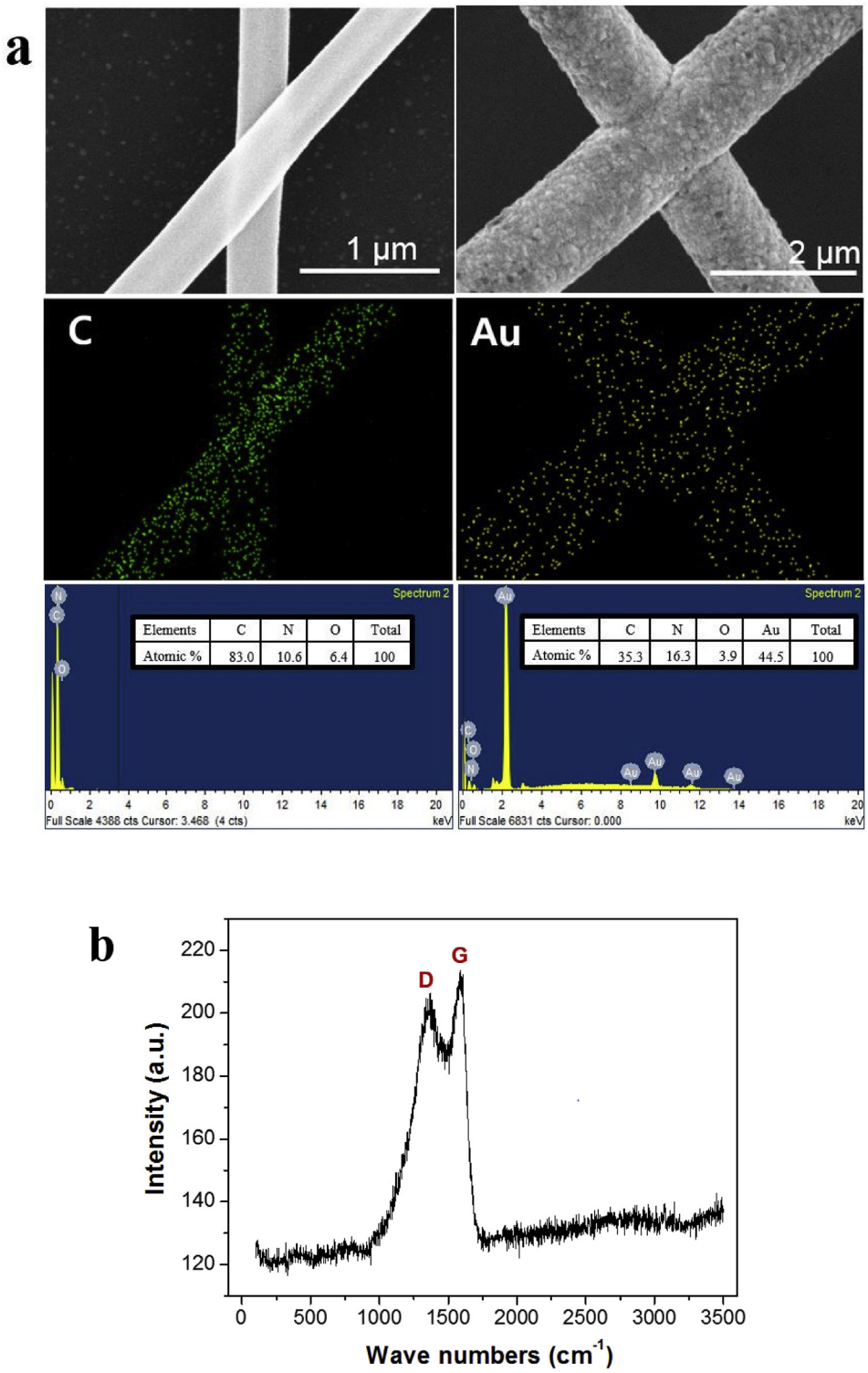

Fig. 3. (a) SEM images, and corresponding EDS elemental mappings and EDS elemental analysis reports of carbon (left) and Au (right) in the CS-CMHMs. (b) Raman spectrum of CS-CMHMs.

percent of light transmitted through the Au-electroplated carbon fiber mats was a bit less than that through the carbon fiber meshes, and we attributed this small decrease to the relatively high coverage by Au coating compared to the carbon fiber nets. In contrast to this small decrease in percent transmittance, the sheet resistance of Au-electroplated carbon fiber mats was dramatically lower than that of the carbon fiber meshes, having been decreased to ~2.7 Ω/sq. We attributed this very considerable decrease in sheet resistance, occurring despite the magnitude of the decrease in percent transmittance being small, to the fiber junction bonding resulting from the plating of the metal on the carbon nanofibers. This optoelectrical performance of CS-CMHMs was comparable to

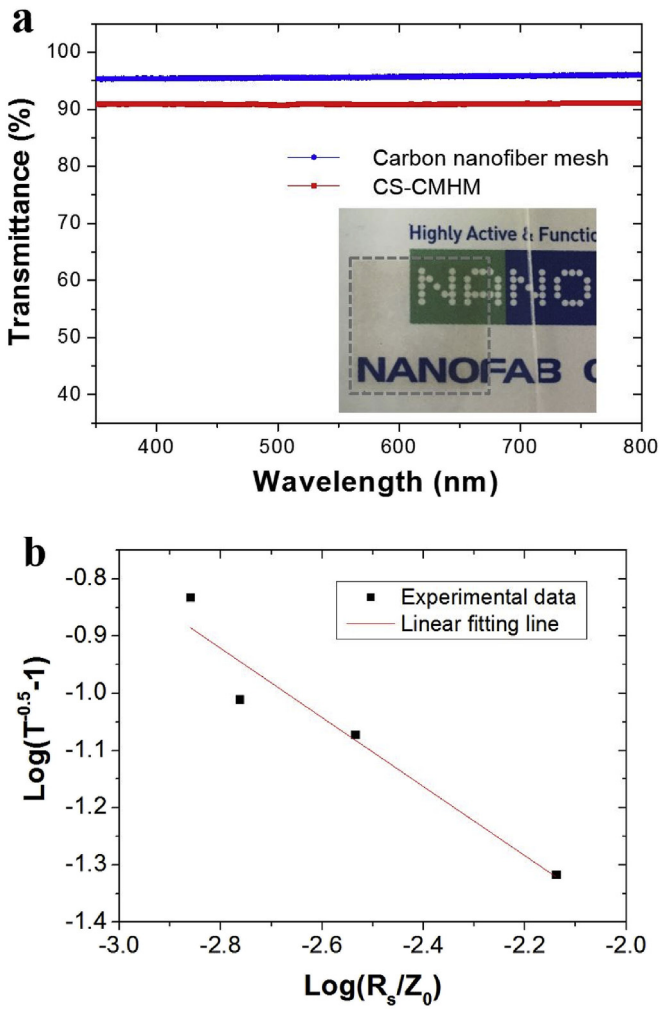

Fig. 4. (a) Transmittance spectra of the carbon nanofiber meshes and the CS-CMHMs on glass substrates. (b) Line fit through the R_s-T performance data of the CS-CMHM films in the percolation regime.

or even better than that of conventional ITO films. Moreover, the percent of light transmitted through the CS-CMHMs did not vary with wavelength over the entire visible range, and such uniform transmittance is highly desirable for optoelectronic devices.

The optoelectronic properties of the CS-CMHMs were found to be well described by percolation theory. The relation between transmittance T and sheet resistance R_S in a percolation network is given by the equation [37]:

$$T = \left[1 + \frac{1}{\Pi}\left(\frac{Z_0}{R_S}\right)^{\frac{1}{(n+1)}}\right]^{-2},$$

where n is the percolation exponent, Z_0 the impedance of free space (377Ω) and Π is the percolation figure-of-merit. This formula shows that high Π and low n values are desired for achieving low R_S coupled with high T, and suggests that the percolation regime can be identified when a log-log plot of $T^{-0.5}-1$ versus R_S/Z_0 is a straight line. The percolation parameters n and Π can be derived from the intercept and slope of a line fitting the data in the log-log plot. Here, all the optoelectronic data obtained from the CS-CMHM films depending on electrospinning time (see Table S1 in supporting information) were fitted using the above formula as shown in Fig. 4b, and this fit was consistent with the performance of the CS-CMHM films having followed percolation theory. From the fitted line, n and Π for the CS-CMHMs were found to be 0.66 and 409, respectively. According to our and other previous reports [37,38], the n value of 0.66 was within the limit expected for true percolation exponents, and the value of Π of CS-CMHMs was found to be 409, greater than the 52, 32, 18, and 3.5 values of Π found for Au nanofiber meshes [38], Ag nanowires, single-walled nanotubes (SWNTs), and graphene [37]. These results indicated the percolation parameters of the CS-CAHMs to be competitive with the values of other nanostructured thin films, and hence proved the high performance of the CS-CMHM films which was due to good interconnection and uniformity of the CS-CMHMs.

To evaluate the flexibility of our CS-CMHM films and hence determine whether they can serve as flexible transparent electrodes, the films were transferred onto a 250-μm-thick polyethylene terephthalate (PET) substrate with an area of 2.5 cm × 2.5 cm. The mechanical stability levels of the CS-CMHM films were examined by carrying out bending tests. Commercialized flexible ITO films were also tested for comparison. As shown in Fig. 5a, the relative increase

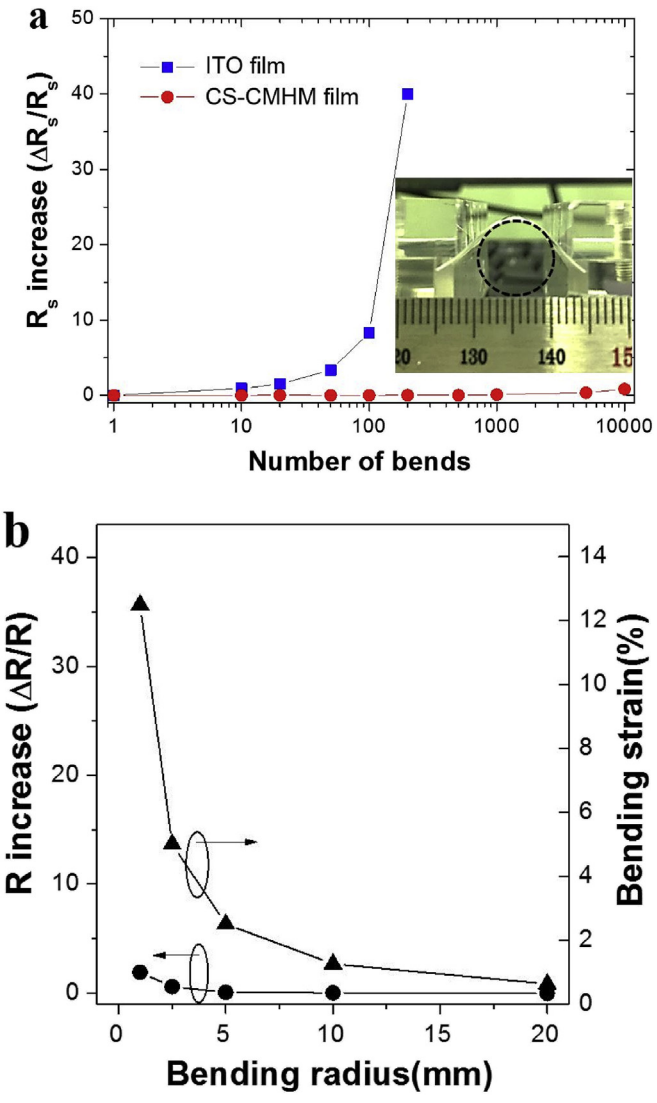

Fig. 5. (a) Relative increase in the sheet resistance (see text for definition) of the ITO film and the CS-CMHM film on respective PET substrates as a function of the number of cycles of repeated bending to a radius of 5 mm. The inset shows a photograph of a CS-CMHM film bent to a bending radius of 5 mm using a bending test system. (b) In situ bending strain (see text for definition) and relative increase in the sheet resistance of CS-CMHM films on respective PET substrates at bending radii of 1, 2.5, 5, 10, 20 mm.

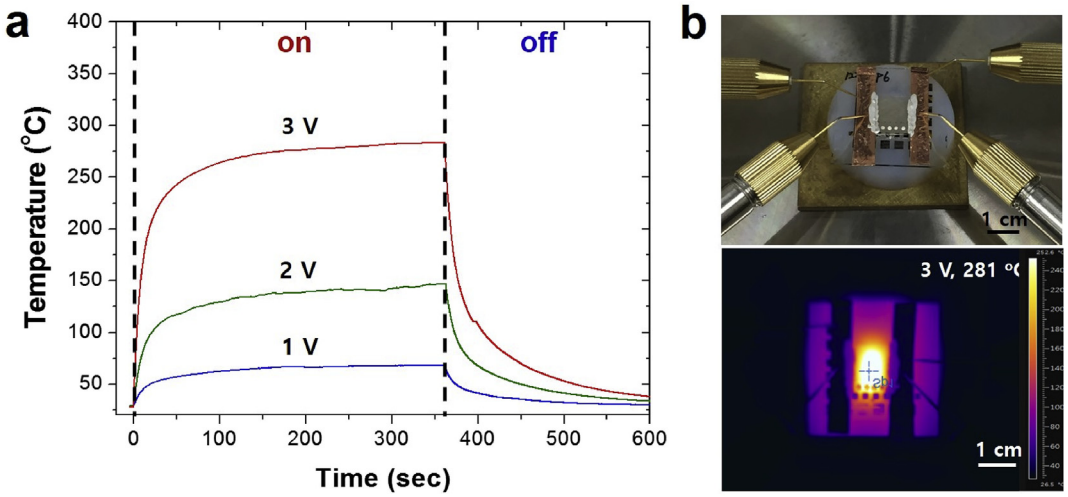

Fig. 6. (a) Temperature profiles of the CS-CMHM films as a function of time for different applied voltages. (b) Photograph (top) and IR image (bottom) of the films undergoing Joule heating using an applied voltage of 3 V.

in the sheet resistance, i.e., $\Delta R_s/R_s$ (defined as the ratio of the sheet resistance (R_s) increase at a bending radius of 5 mm to the initial sheet resistance), of the CS-CMHM films after 1000 cycles of bending was measured to be only ~ 0.1 (from the initial sheet resistance of ~2–3 Ω/sq). Even after 10000 bending cycles, the films maintained their electrical conductivity, implying superb functional flexibility of the CS-CMHM electrodes. In contrast, the ITO film exhibited an increased resistance (Fig. 5a) as well as a drastic decrease in conductance after just a few bending cycles. The mechanical stability levels of bent CS-CMHM films with bending radii of 1, 2.5, 5, 10, and 20 mm were also evaluated, by taking resistance measurements in situ. At each bending radius value, all samples were bent, and the resistance was monitored in conjunction with bending. Fig. 5b shows the bending strain (ε) and the relative increase in sheet resistance of CS-CMHM films bent to the above various bending radii. Here, bending strain was calculated using the formula $\varepsilon = d/(2r)$, where d is the substrate thickness, and r is the bending radius. No severe decrease in conductance was observed up to a bending radius of ~1 mm, corresponding to a bending strain (ε) of 12.5%. The results of the bending test showed the mechanical stability of our CS-CMHM films to be superior to those of previously reported flexible transparent films [26–28]. These results can be attributed to the strong bonding between the fibers at their junctions, with this strong bonding having arisen from the new junctions formed between fibers as a result of the metal electroplating as well as having arisen from the connections already existing between the electrospun carbon fiber templates. These results indicate the potential use of CS-CMHM films as flexible transparent electrodes.

Transparent electrodes using CS-CMHM films can be used as transparent heaters. The Joule heating characteristics of the films were investigated by applying various constant voltages (1, 2, or 3 V) for six minutes, and for each of these three experiments measuring the temperature of the film throughout this duration of time (Fig. 6a). To carry out these experiments, the area of each of the tested mesh films was made to be 1.0 cm × 1.0 cm, the films were transferred to respective glass substrates, and Ag paste was coated on both ends of the films to connect them to the voltage supplier (Fig. 6b). Upon applying the various voltages, the temperatures of each of the films increased rapidly and then gradually leveled off, at about 67 °C (for the application of 1 V), 145 °C (for 2 V), and 281 °C (for 3 V). Generally, the overall Joule heat (H) emitted by a heater during time T is given by $H = IVT$, where I is the electric current; also, $I = V/R$, where R is the total resistance. Namely, to achieve a high electric current at a given applied voltage, R should be low. Therefore, the CS-CMHM-based film heater with a low sheet resistance of ~2–3 Ω/sq requires only a low voltage to yield a high temperature, indicating the low power consumption of the heater. With an applied voltage of 3 V, the temperature rose to above 200 °C within an extremely short period of time (less than 20 s) and then fairly soon thereafter to ~280 °C. Even after joule heating to ~280 °C, the CS-CMHM networks maintained favorable condition without degradation (see Fig. S3 in supporting information). These heating properties of the CS-CMHM films were superior to those of other metallic nanofiber mesh films [12], with this superiority attributed to the high thermal conductivity of the carbon nanofibers in the inner core of the CS-CMHNs. Moreover, carbon fibers also have a very low coefficient of thermal expansion; hence, CS-CMHM films hybridized with carbon nanofibers have the advantage of exhibiting high tolerance in heating applications.

4. Conclusions

In this work, electrospinning and electroplating were used to fabricate films composed of a metal layer covering conductive carbon fiber mesh structures, and these films demonstrated potential for use as flexible transparent electrodes. Conductive carbon nanofiber templates were easily prepared by applying a heat treatment to electrospun polymer precursors. Au layers were uniformly coated on the carbon nanofiber templates by carrying out electroplating, which enabled the spontaneous formation of highly-fused junctions at the intersection of the fibers and yielded a remarkable reduction of the contact resistance at these junctions. These carbon-hybridized metal meshes, denoted as CS-CMHMs, formed fibers with diameters of ~1 μm, transmitted ~91% of visible light, showed a low sheet resistance of ~2.7 Ω/sq, and displayed excellent mechanical stability even after 10000 cycles of bending the films to a radius of 5 mm. In addition, these films showed superb Joule heating properties for heater applications: applying a voltage of only 3 V to these films resulted in a very rapid increase in their surface temperature, which in relatively short order then reached ~280 °C. These advantageous heating properties of the CS-CMHM films were due to their high levels of electrical and thermal conductivity. Based on these results, the CS-CMHM films and the process used to fabricate them are expected to find use in high-performance flexible transparent electrodes and their applications.

Acknowledgements

This research was supported by Leading Foreign Research Institute Recruitment Program (NRF-2015K1A4A3047100), Global Frontier Program (NRF-2015M3A6B3068660), and Nano R&D Program (NRF-2015M3A787046618) through the National Research Foundation of Korea (NRF) funded by the Ministry of Education, Science and Technology (MEST). This work was supported by the National Research Foundation of Korea (NRF) grant funded by the Korea government (Ministry of Science, ICT and Future Planning) (NRF-2017R1C1B1006807).

Appendix A. Supplementary data

Supplementary data related to this article can be found at http://dx.doi.org/10.1016/j.cap.2017.07.016.

References

[1] S. Bae, H. Kim, Y. Lee, X. Xu, J.-S. Park, Y. Zheng, J. Balakrishnan, T. Lei, H.R. Kim, Y.I. Song, Roll-to-roll production of 30-inch graphene films for transparent electrodes, Nat. Nanotechnol. 5 (2010) 574–578.
[2] S. Tsuyoshi, N. Hiroyoshi, M. Hiroki, F. Takanori, A. Takuzo, H. Kenji, S. Takao, Stretchable active-matrix organic light-emitting diode display using printable elastic conductors, Nat. Mater. 8 (2009) 494–499.
[3] J. Li, L. Hu, L. Wang, Y. Zhou, G. Gruner, T.J. Marks, Organic light-emitting diodes having carbon nanotube anodes, Nano Lett. 6 (2006) 2472–2477.
[4] Z. Yu, L. Li, Q. Zhang, W. Hu, Q. Pei, Silver nanowire-polymer composite electrodes for efficient polymer solar cells, Adv. Mater. 23 (2011) 4453–4457.
[5] G.P. Kushto, W. Kim, Z.H. Kafafi, Flexible organic photovoltaics using conducting polymer electrodes, Appl. Phys. Lett. 86 (2005) 093502.
[6] J.W. Kim, H.-J. Jeon, C.-L. Lee, C.W. Ahn, Fabrication of three-dimensional nanostructure-embedded ITO and its application as a transparent electrode for high-efficiency solution processable organic photovoltaic devices, Nanoscale 9 (2017) 3033–3039.
[7] D.J. Lipomi, M. Vosgueritchian, B.C.-K. Tee, S.L. Hellstrom, J.A. Lee, C.H. Fox, Z. Bao, Skin-like pressure and strain sensors based on transparent elastic films of carbon nanotubes, Nat. Nanotechnol. 6 (2011) 788–792.
[8] B.W. An, B.G. Hyun, S.-Y. Kim, M. Kim, M.-S. Lee, K. Lee, J.B. Koo, H.Y. Chu, B.-S. Bae, J.-U. Park, Stretchable and transparent electrodes using hybrid structures of graphene-metal nanotrough networks with high performances and ultimate uniformity, Nano Lett. 14 (2014) 6322–6328.
[9] J.-K. Song, D. Son, J. Kim, Y.J. Yoo, G.J. Lee, L. Wang, M.K. Choi, J. Yang, M. Lee, K. Do, J.H. Koo, N. Lu, J.H. Kim, T. Hyeon, Y.M. Song, D.H. Kim, Wearable force touch sensor array using a flexible and transparent electrode, Adv. Func. Mater. 27 (2017) 1605286.
[10] H.-J. Jeon, J.Y. Kim, W.-B. Jung, H.-S. Jeong, Y.H. Kim, D.O. Shin, S.-J. Jeong, J. Shin, S.O. Kim, H.-T. Jung, Complex high-aspect-ratio metal nanostructures by secondary sputtering combined with block copolymer self-assembly, Adv. Mater. 28 (2016) 8439–8445.
[11] R.G. Gordon, Criteria for choosing transparent conductors, MRS Bull. 25 (2000) 52–57.
[12] B.W. An, E.-J. Gwak, K. Kim, Y.-C. Kim, J. Jang, J.-Y. Kim, J.-U. Park, Stretchable, transparent electrodes as wearable heaters using nanotrough networks of metallic glasses with superior mechanical properties and thermal stability, Nano Lett. 16 (2016) 471–478.
[13] Z. Wu, Z. Chen, X. Du, J.M. Logan, J. Sippel, M. Nikolou, K. Kamaras, J.R. Reynolds, D. Tanner, A.F. Hebard, A.G. Rinzler, Transparent, conductive carbon nanotube films, Science 305 (2004) 1273–1276.
[14] D.S. Hecht, L. Hu, G. Irvin, Emerging transparent electrodes based on thin films of carbon nanotubes, graphene, and metallic nanostructures, Adv. Mater. 23 (2011) 1482–1513.
[15] H. Sirringhaus, T. Kawase, R.H. Friend, T. Shimoda, M. Inbasekaran, W. Wu, E.P. Woo, High-resolution inkjet printing of all-polymer transistor circuits, Science 290 (2000) 2123–2126.
[16] J.W. Huh, Y.M. Kim, Y.W. Park, J.H. Choi, J.W. Lee, J.W. Lee, J.W. Yang, S.H. Ju, K.K. Paek, B.K. Ju, Characteristics of organic light-emitting diodes with conducting polymer anodes on plastic substrates, J. Appl. Phys. 103 (2008) 044502.
[17] M. Vosgueritchian, D.J. Lipomi, Z. Bao, Highly conductive and transparent PEDOT: PSS films with a fluorosurfactant for stretchable and flexible transparent electrodes, Adv. Funct. Mater. 22 (2012) 421–428.
[18] X. Li, G. Zhang, X. Bai, X. Sun, X. Wang, E. Wang, H. Dai, Highly conducting graphene sheets and Langmuir-Blodgett films, Nat. Nanotechnol. 3 (2008) 538–542.
[19] G. Eda, G. Fanchini, M. Chhowalla, Large-area ultrathin films of reduced graphene oxide as a transparent and flexible electronic material, Nat. Nanotechnol. 3 (2008) 270–274.
[20] K.S. Kim, Y. Zhao, H. Jang, S.Y. Lee, J.M. Kim, K.S. Kim, J. Ahn, P. Kim, J. Choi, B.H. Hong, Large-scale pattern growth of graphene films for stretchable transparent electrodes, Nature 457 (2009) 706–710.
[21] J.-Y. Lee, S.T. Connor, Y. Cui, P. Peumans, Solution processed metal nanowire mesh transparent electrodes, Nano Lett. 8 (2008) 689–692.
[22] S. De, T. Higgins, P.E. Lyons, E.M. Doherty, P.N. Nirmalraj, W.J. Blau, J.J. Boland, J.N. Coleman, Silver nanowire networks as flexible, transparent, conducting films: extremely high DC to optical conductivity ratios, ACS Nano 3 (2009) 1767–1774.
[23] A.R. Rathmell, S.M. Bergin, Y.L. Hua, Z.Y. Li, B.J. Wiley, The growth mechanism of copper nanowires and their properties in flexible, transparent conducting films, Adv. Mater 22 (2010) 3558–3563.
[24] H. Wu, L. Hu, M.W. Rowell, D. Kong, J.J. Cha, J.R. McDonough, J. Zhu, Y. Yang, M.D. McGehee, Y. Cui, Electrospun metal nanofiber webs as high-performance transparent electrode, Nano Lett. 10 (2010) 4242–4248.
[25] P.C. Hsu, H. Wu, T.J. Carney, M.T. McDowell, Y. Yang, E.C. Garnett, M. Li, L. Hu, Y. Cui, Passivation coating on electrospun copper nanofibers for stable transparent electrodes, ACS Nano 6 (2012) 5150–5156.
[26] H. Wu, D. Kong, Z. Ruan, P.-C. Hsu, S. Wang, Z. Yu, T.J. Carney, L. Hu, S. Fan, Y. Cui, Transparent electrode based on a metal nanotrough network, Nat. Nanotechnol. 8 (2013) 421–425.
[27] P.-C. Hsu, S. Wang, H. Wu, V.K. Narasimhan, D. Kong, H.R. Lee, Y. Cui, Performance enhancement of metal nanowire transparent conducting electrodes by mesoscale metal wires, Nat. Commun. 4 (2013) 1–7.
[28] S. An, H.S. Jo, D.-Y. Kim, H.J. Lee, B.-K. Ju, S.S. Al-Deyab, J.-H. Ahn, Y. Qin, M.T. Swihart, A.L. Yarin, S.S. Yoon, Self-junctioned copper nanofiber transparent flexible conducting film via electrospinning and electroplating, Adv. Mater. 28 (2016) 7149–7154.
[29] C.H. Seager, G.E. Pike, Phys. Rev. B 10 (1974) 1435–1446.
[30] M.S.A. Rahaman, A.F. Ismail, A. Mustafa, A review of heat treatment on polyacrylonitrile fiber, Polym. Degrad. Stab. 92 (2007) 1421–1432.
[31] T.K. Ko, Influence of continuous stabilization on the physical properties and microstructure of PAN-based carbon fibers, Appl. Polym. Sci. 42 (1991) 1949–1957.
[32] P. Rangarajan, V.A. Bhanu, D. Godshall, G.L. Wikels, J.E. McGrath, D.G. Baird, Dynamic oscillatory shear properties of potentially melt processable high acrylonitrile terpolymers, Polymer 43 (2002) 2699–2709.
[33] T.H. Ko, The Influence of pyrolysis on physical properties and microstructure of modified PAN fibers during carbonization, Appl. Polym. Sci. 43 (1991) 589–600.
[34] R.B. Mathur, T.L. Dhami, O.P. Bahl, Shrinkage behaviour of modified PAN precursors-its influence on the properties of resulting carbon fibre, Polym. Degrad. Stab. 14 (1986) 179–187.
[35] J. Mittal, R.B. Mathur, O.P. Bahl, Single step carbonization and graphitization of highly stabilized PAN fibers, Carbon 35 (1997) 1196–1197.
[36] M. Trinquecoste, J.L. Carlier, A. Derrb, P. Delhaes, P. Chadeyron, High temperature thermal and mechanical properties of high tensile carbon single filaments, Carbon 34 (1996) 923–929.
[37] S. De, P.J. King, P.E. Lyons, U. Khan, J.N. Coleman, Size effects and the problem with percolation in nanostructured transparent conductors, ACS Nano 4 (2010) 7064–7072.
[38] J.W. Huh, D.K. Lee, H.-J. Jeon, C.W. Ahn, New approach for fabricating hybrid-structured metal mesh films for flexible transparent electrodes by the combination of electrospinning and metal deposition, Nanotechnology 27 (2016) 4753029.